

## Enhanced Second Harmonic Generation on Passing from a Mono- to a Dicopper(II) Bis(salicylaldiminato) Schiff Base Complex

Frédéric Averseng, Pascal G. Lacroix,\* Isabelle Malfant, Nicolas Périssé, and Christine Lepetit

Laboratoire de Chimie de Coordination du CNRS, 205 route de Narbonne, 31077 Toulouse, France

Keitaro Nakatani

PPSM-UMR 8531, Ecole Normale Supérieure de Cachan, Avenue du Président Wilson, 94235 Cachan, France

Received November 28, 2000

A new ligand (H<sub>2</sub>LOH) obtained from the Schiff base condensation of 4-(diethylamino)salicylaldehyde with 1,3-diamino-2-propanol is reported, which yields two different copper(II) complexes: CuLOH and Cu<sub>2</sub>LO(AcO). Crystal data are as follows. CuLOH·EtOH: monoclinic,  $P2_1/n$ ,  $a = 17.810(2)$  Å,  $b = 8.515(1)$  Å,  $c = 18.912(2)$  Å,  $\beta = 112.72(1)^\circ$ ,  $Z = 4$ . Cu<sub>2</sub>LO(AcO)·1/2H<sub>2</sub>O: monoclinic,  $P2_1/c$ ,  $a = 21.407(4)$  Å,  $b = 15.308(2)$  Å,  $c = 20.156(3)$  Å,  $\beta = 116.83(2)^\circ$ ,  $Z = 4$ . Cu<sub>2</sub>LO(AcO)·1/2 H<sub>2</sub>O is antiferromagnetically coupled with  $J = -207.7$  cm<sup>-1</sup> ( $J$  being the parameter of the exchange Hamiltonian  $H = -J S_A \cdot S_B$ ). CuLOH and Cu<sub>2</sub>LO(AcO) exhibit good transparencies in the visible frequency range with absorption maxima at 353 and 372 nm, respectively. An enhancement of 83% of the quadratic hyperpolarizability ( $\beta$ ) is observed by the electric field induced second harmonic (EFISH) technique on passing from the mono- to the dinuclear species. Qualitative ZINDO/SCI quantum-chemical predictions give a satisfactory account for this enhancement. The spin dependence of the NLO response of Cu<sub>2</sub>LO(AcO)·1/2H<sub>2</sub>O is found to be negligible within the framework of the DFT theory.

### Introduction

The elaboration of molecular materials with large quadratic nonlinear optical (NLO) properties has attracted considerable interest for the past two decades because of their potential applications in photonic devices, such as frequency doublers and electrooptic modulators.<sup>1,2</sup> Many donor–acceptor substituted  $\pi$ -conjugated organics exhibiting large molecular hyperpolarizabilities ( $\beta$ ) have been investigated in the substituted stilbene,<sup>3</sup> thiophene-based stilbene,<sup>4</sup> and polyenes<sup>5</sup> series. Various organometallic chromophores have also been reported.<sup>6</sup>

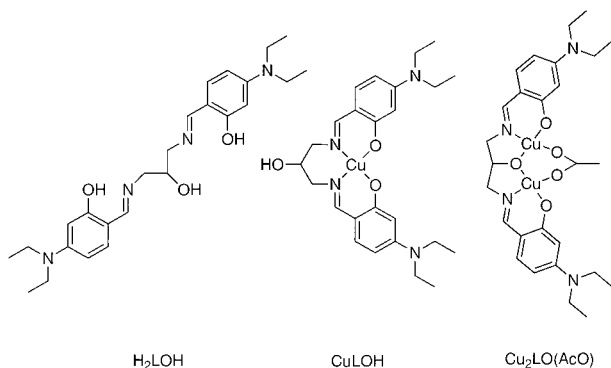
By contrast, few studies have been devoted to inorganic molecules.<sup>7</sup> Most of them have focused on bipyridine<sup>8</sup> and Schiff base metal complexes<sup>9,10</sup> or push–pull arylethynyl porphyrins.<sup>11</sup> Compared to the more common organic molecules, inorganic chromophores offer a large variety of novel structures, the possibility of enhanced thermal stability, and a diversity of tunable electronic behaviors by virtue of the coordination metal center which might bring about NLO materials with unique characteristics such as electrochemical or magnetic properties.<sup>12,13</sup>

We, and others, have recently reported on a family of bis(salicylaldiminato) metal Schiff base complexes with sizable  $\beta$

- (1) (a) Prasad, P. N.; Williams, D. J. *Introduction to Nonlinear Optical Effects in Molecules and Polymers*; J. Wiley: Chichester, 1991. (b) *Molecular Nonlinear Optics: Materials, Physics, and Devices*; Zyss, J., Ed.; Academic Press: New York, 1994. (c) *Nonlinear Optics of Organic Molecules and Polymers*; Nalwa, H. S., Miyata, S., Eds.; CRC Press: New York, 1997.
- (2) (a) Dalton, L. R.; Harper, A. W.; Ghosn, R.; Steier, W. H.; Ziari, M.; Fetterman, H.; Shi, Y.; Mustacich, R. V.; Jen, A. K.-Y.; Shea, K. J. *Chem. Mater.* **1995**, *7*, 1060. (b) Benning, R. G. *J. Mater. Chem.* **1995**, *5*, 365. (c) Optical nonlinearities in Chemistry (Burland, D. M., Ed.), special issue of *Chem. Rev.* **1994**, *94* (1). (d) Verbiest, T.; Houbrechts, S.; Kauranen, M.; Clays, K.; Persoons, A. *J. Mater. Chem.* **1997**, *7*, 2175.
- (3) (a) Cheng, L. T.; Tam, W.; Stevenson, S. H.; Meredith, G. R.; Rikken, G.; Marder, S. R. *J. Phys. Chem.* **1991**, *95*, 10631. (b) Cheng, L. T.; Tam, W.; Marder, S. R.; Stiegman, A. E.; Rikken, G.; Spangler, C. W. *J. Phys. Chem.* **1991**, *95*, 10643.
- (4) (a) Pushkara Rao, V.; Jen, A. K.-Y.; Chandrasekhar, J.; Nambhothiri, I. N.; Rathna, A. *J. Am. Chem. Soc.* **1996**, *118*, 12443. (b) Jen, A. K.-Y.; Pushkara Rao, V.; Wong, K. Y.; Drost, K. J. *J. Chem. Soc., Chem. Commun.* **1993**, 90.
- (5) (a) Blanchard-Desce, M.; Alain, V.; Bedworth, P. V.; Marder, S. R.; Fort, A.; Runser, C.; Barzoukas, M.; Lebus, S.; Wortmann, R. *Chem. Eur. J.* **1997**, *3*, 1091. (b) Blanchard-Desce, M.; Bloy, V.; Lehn, J.-M.; Runser, C.; Barzoukas, M.; Fort, A.; Zyss, J. *SPIE Proc.* **1994**, *2143*, 20.

- (6) (a) Cheng, L. T.; Tam, W.; Meredith, G. R.; Marder, S. R. *Mol. Cryst. Liq. Cryst.* **1990**, *189*, 137. (b) Marder, S. R. In *Inorganic Materials*; Bruce, D. O'Hare, W. D., Eds.; John Wiley & Sons: New York, 1992; p 115. (c) Long, N. J. *Angew. Chem., Int. Ed. Engl.* **1995**, *34*, 21. (d) Whittall, I. R.; McDonagh, A. M.; Humphrey, M. G.; Samoc, M. *Adv. Organomet. Chem.* **1998**, *42*, 291.
- (7) For a recent general review, see ref 2d.
- (8) Le Bozec, H.; Renouard, T. *Eur. J. Inorg. Chem.* **2000**, 229.
- (9) (a) Di Bella, S.; Fragalà, I.; Ledoux, I.; Diaz-Garcia, M. A.; Lacroix, P. G.; Marks, T. J. *Chem. Mater.* **1994**, *6*, 881. (b) Di Bella, S.; Fragalà, I.; Ledoux, I.; Marks, T. J. *J. Am. Chem. Soc.* **1995**, *117*, 9481. (c) Di Bella, S.; Fragalà, I.; Ledoux, I.; Diaz-Garcia, M. A.; Marks, T. J. *J. Am. Chem. Soc.* **1997**, *119*, 9550.
- (10) (a) Lacroix, P. G.; Di Bella, S.; Ledoux, I. *Chem. Mater.* **1996**, *8*, 541. (b) Lenoble, G.; Lacroix, P. G.; Daran, J. C.; Di Bella, S.; Nakatani, K. *Inorg. Chem.* **1998**, *37*, 2158. (c) Averseng, F.; Lacroix, P. G.; Malfant, I.; Lenoble, G.; Cassoux, P.; Nakatani, K.; Maltey-Fanton, I.; Delaire, J.; Aukauloo, A. *Chem. Mater.* **1999**, *11*, 995. (d) Averseng, F.; Lacroix, P. G.; Malfant, I.; Dahan, I.; Nakatani, K. *J. Mater. Chem.* **2000**, *10*, 1013.
- (11) (a) LeCours, S. M.; Guan, H.-W.; DiMaggio, S. G.; Wang, C. H.; Therien, M. J. *J. Am. Chem. Soc.* **1996**, *118*, 1497. (b) Priyadarshy, S.; Therien, M. J.; Beratan, D. N. *J. Am. Chem. Soc.* **1996**, *118*, 1504.

## Scheme 1



values and high thermal stabilities.<sup>9,10</sup> The first investigations were devoted to diamagnetic square planar nickel(II) derivatives, which allowed a simplified but fruitful quantum description of the NLO responses. Later on, Di Bella et al. reported that changing the nature of the metal to a paramagnetic ion (e.g.,  $\text{Cu}^{\text{II}}$  or  $\text{Co}^{\text{II}}$ ) could enhance the  $\beta$  values.<sup>9b</sup> Additional investigations have also implemented the idea that unpaired electrons could lead to large NLO response, for instance, in radicals<sup>14,15</sup> or in an iron(II) metal complex upon spin transition ( $S = 0 \rightarrow 2$ ).<sup>16</sup>

To further explore the potential capabilities of paramagnetic complexes in the design of NLO materials, and in a research effort aimed at extending the range and electronic properties of inorganic systems, we report here on the first investigation of the NLO properties of a magnetically coupled dinuclear metal complex. The mononuclear  $\text{CuLOH}$  and the dinuclear  $\text{Cu}_2\text{LO}(\text{AcO})$  derivatives are presented in Scheme 1 with their related  $\text{H}_2\text{LOH}$  ligand. The present study focuses on the synthesis, crystal structures, and comparison of the quadratic NLO properties of both metal complexes. The origin of the enhancement of the NLO response observed on passing from the mono- to the dinuclear species is discussed within the framework of the intermediate neglect of differential overlap (INDO) formalism. Finally, the magnetic coupling occurring within the  $\text{Cu}_2\text{LO}(\text{AcO})$  entity is presented and the possibility for spin dependence of  $\beta$  is examined.

## Experimental Section

**Starting Materials and Equipment.** 1,3-Diamino-2-propanol (Aldrich), 4-(diethylamino)salicylaldehyde (Aldrich),  $\text{Cu}^{\text{II}}(\text{AcO})_2 \cdot \text{H}_2\text{O}$  (Aldrich), and the solvents (SDS or Carlo Erba) for the spectroscopic studies were used without further purification.  $^1\text{H}$  NMR spectra were recorded on a Bruker AM 250 spectrometer and the UV-visible spectra on a Hewlett-Packard 8452 A spectrophotometer. Elemental analyses were performed by the Service de Microanalyses du C.N.R.S., Laboratoire de Chimie de Coordination, Toulouse. Thermal measurements were performed by TG/DTA (thermogravimetric/differential thermoanalysis) on a Setaram-TGDTA92 thermoanalyzer. The experiments were conducted under nitrogen on about 5 mg of sample (heating rate:  $10^\circ\text{C min}^{-1}$ ).

**Ligand ( $\text{H}_2\text{LOH}$ ) Synthesis.** A solution of 0.3 g ( $3.33 \times 10^{-3}$  mol) of 1,3-diamino-2-propanol and 1.284 g ( $6.64 \times 10^{-3}$  mol) of 4-(diethylamino)salicylaldehyde in 50 mL of ethanol was refluxed for 1 week. The resulting solution was concentrated to 5 mL and poured into 100 mL of cold  $\text{Et}_2\text{O}$ , which gave 1.41 g (95% yield) of a yellow precipitate. The compound was filtered, washed with  $\text{Et}_2\text{O}$ , and dried under vacuum.  $^1\text{H}$  NMR ( $\text{CDCl}_3$ ),  $\delta$ : 1.15 (t,  $J = 7.1$  Hz, 12H), 3.34 (q,  $J = 7.1$  Hz, 8H), 3.55–3.75 (m, 4H), 4.11 (m, 1H), 6.08 (d,  $J = 2.0$  Hz, 2H), 6.13 (d,  $J = 8.8$  Hz, 2H), 6.99 (d,  $J = 8.6$  Hz, 2H), 8.03 (s, 2H). Anal. Calcd (Found) for  $\text{C}_{25}\text{H}_{36}\text{N}_4\text{O}_3$ : C, 68.15 (67.96); H, 8.24 (7.89); N, 12.72 (12.54).

**Complexes Synthesis.** (a)  $\text{CuLOH} \cdot \text{C}_2\text{H}_5\text{OH}$ . In a solution of 1.1 g ( $2.5 \times 10^{-3}$  mol) of  $\text{H}_2\text{LOH}$  in 25 mL of ethanol was added 454 mg ( $2.5 \times 10^{-3}$  mol) of  $\text{Cu}(\text{AcO})_2 \cdot \text{H}_2\text{O}$  dissolved in 25 mL of EtOH. The resulting solution was refluxed for 24 h. Cooling down to  $-10^\circ\text{C}$  afforded 780 mg (75% yield) of a yellow green microcrystalline powder. The compound was filtered, washed with cold ethanol, and dried in a desiccator. Anal. Calcd (Found) for  $\text{C}_{25}\text{H}_{34}\text{CuN}_4\text{O}_3 \cdot \text{C}_2\text{H}_5\text{OH}$ : C, 59.16 (59.20); H, 7.35 (7.21); N, 10.22 (10.09). Single crystals suitable for X-ray analysis were obtained as green plates by slow evaporation in ethanol.

(b)  $\text{Cu}_2\text{LO}(\text{AcO}) \cdot \frac{1}{2}\text{H}_2\text{O}$ . In a solution of 660 mg ( $1.5 \times 10^{-3}$  mol) of  $\text{H}_2\text{LOH}$  in 20 mL of ethanol was added 600 mg ( $3 \times 10^{-3}$  mol) of  $\text{Cu}(\text{AcO})_2 \cdot \text{H}_2\text{O}$  dissolved in 30 mL of ethanol. After dropwise addition of 460 mg ( $4.5 \times 10^{-3}$  mol) of triethylamine, the resulting solution was refluxed for 24 h, then concentrated to  $\frac{1}{3}$  of its initial volume, and cooled to  $-10^\circ\text{C}$ . A yellow green precipitate (750 mg, 70% yield) was filtered, washed with cold ethanol, and dried in a desiccator. Anal. Calcd (Found) for  $\text{C}_{27}\text{H}_{36}\text{Cu}_2\text{N}_4\text{O}_5 \cdot \frac{1}{2}\text{H}_2\text{O}$ : C, 51.26 (51.27); H, 5.89 (5.96); N, 8.85 (8.54). Single crystals suitable for X-ray analysis were obtained as green plates by slow evaporation in ethanol.

**X-ray Crystal Structure Determination.** The data were collected at 160 K on a Stoe Imaging Plate Diffraction System (IPDS) equipped with an Oxford Cryosystems cooler device, with a tube power of 1.5 kW (50 kV, 30 mA). The crystal-to-detector distance was 80 mm. A total of 167 exposures (1.5 min per exposure) were obtained with  $0 < \varphi < 250.5^\circ$  and with the crystals rotated through  $1.5^\circ$  in  $\varphi$ .

The structures were solved by direct methods (Shelxs-86)<sup>17</sup> and refined by least-squares procedures on  $F_{\text{obs}}$ . Hydrogen atoms were introduced in the calculation in idealized positions ( $d(\text{CH}) = 0.99 \text{ \AA}$ ) and their atomic coordinates were recalculated after each cycle. They were given isotropic thermal parameters 20% higher than those of the carbon to which they are attached. Least-squares refinements were carried out by minimizing the function  $\sum w(|F_o| - |F_c|)^2$ , where  $F_o$  and  $F_c$  are the observed and calculated structure factors. The weighting scheme used in the last refinement cycles was  $w = w'[1 - (\Delta F/6\sigma(F_o))^2]^2$ , where  $w' = 1/\sum_i^n A_i T_i(x)$  with the Chebyshev polynomial  $A_i T_i(x)$  where  $x$  is  $F_o/F_c(\text{max})$ .<sup>18</sup> Five coefficients ( $A_1 = 2.240, -0.893, 2.007, -0.475, 0.364$ ) were used for  $\text{CuLOH} \cdot \text{C}_2\text{H}_5\text{OH}$ , and three coefficients ( $A_1 = 3.660, 0.255, 3.060$ ) for  $\text{Cu}_2\text{LO}(\text{AcO}) \cdot \frac{1}{2}\text{H}_2\text{O}$ . Models reached convergence with  $R = \sum(|F_o| - |F_c|)/\sum|F_o|$  and  $R_w = \sum w(|F_o| - |F_c|)^2/\sum w(F_o)^2$ , having values listed in Table 1. Criteria for a satisfactory complete analysis were the ratios of rms shift to standard deviation less than 0.1 and no significant features in final difference maps. Details of data collection and refinement are given in Table 1. In  $\text{CuLOH} \cdot \text{C}_2\text{H}_5\text{OH}$ , a disorder of the hydroxy substituent was refined anisotropically on two positions with occupancies of 0.50/0.50.

The calculations were carried out with the CRYSTALS package programs<sup>19</sup> running on a PC. The drawing of the molecules was realized with the help of CAMERON.<sup>20</sup> Full interatomic distances and bond angles, fractional atomic coordinates, and the equivalent thermal

(12) (a) Geoffroy, G. L.; Wrighton, M. S. *Organometallic Photochemistry*; Academic Press: New York, 1979. (b) Collman, J. P.; Hegedus, L. S. *Principles and Applications of Organotransition Metal Chemistry*; University Science Books: Mill Valley, CA, 1987.  
 (13) Kahn, O. *Molecular Magnetism*; VCH Publishers: New York, 1993.  
 (14) Di Bella, S.; Fragalà, I.; Marks, T. J.; Ratner, M. A. *J. Am. Chem. Soc.* **1996**, *118*, 12747.  
 (15) Malfant, I.; Cordente, N.; Lacroix, P. G.; Lepetit, C. *Chem. Mater.* **1998**, *10*, 4079.  
 (16) Averseng, F.; Lacroix, P. G.; Lepetit, C.; Tuchagues, J. P. *Chem. Mater.* **2000**, *12*, 2225.

(17) Sheldrick, G. M. *SHELXS86, Program for Crystal Structure Solution*; University of Göttingen: Göttingen, Germany, 1986.  
 (18) Prince, E. *Mathematical Techniques in Crystallography*; Springer-Verlag: Berlin, 1982.  
 (19) Watkin, D. J.; Prout, C. K.; Carruthers, J. R.; Betteridge, P. W. *CRYSTALS Issue 10*; Chemical Crystallography Laboratory, University of Oxford: Oxford, 1996.

**Table 1.** Crystal Data for CuLOH·EtOH, and Cu<sub>2</sub>LO(AcO)·<sup>1</sup>/<sub>2</sub>H<sub>2</sub>O

	CuLOH·EtOH	Cu <sub>2</sub> LO(AcO)· <sup>1</sup> / <sub>2</sub> H <sub>2</sub> O
chemical formula	C <sub>27</sub> H <sub>40</sub> CuN <sub>4</sub> O <sub>4</sub>	C <sub>27</sub> H <sub>37</sub> Cu <sub>2</sub> N <sub>4</sub> O <sub>11/2</sub>
crystal form	elongated plate	elongated plate
crystal size (mm)	0.375 × 0.1 × 0.02	0.3 × 0.1 × 0.02
<i>a</i> (Å)	17.810(2)	21.407(4)
<i>b</i> (Å)	8.515(1)	15.308(2)
<i>c</i> (Å)	18.912(2)	20.156(3)
$\beta$ (deg)	112.72(1)	116.83(2)
<i>V</i> (Å <sup>3</sup> )	2645.6	5894.0
<i>Z</i>	4	4
fw (g mol <sup>-1</sup> )	548.16	1265.39
space group	<i>P</i> 2 <sub>1</sub> / <i>n</i>	<i>P</i> 2 <sub>1</sub> / <i>c</i>
<i>T</i> (K)	160	160
radiation	Mo K $\alpha$ (0.71069 Å)	Mo K $\alpha$ (0.71069 Å)
$\rho_{\text{calcd}}$ (g cm <sup>-3</sup> )	1.369	1.426
$\mu$ (cm <sup>-1</sup> )	8.637	14.882
absorption correction	numerical	numerical
	<i>T</i> <sub>min</sub> = 0.7466	<i>T</i> <sub>min</sub> = 0.6260
	<i>T</i> <sub>max</sub> = 0.8612	<i>T</i> <sub>max</sub> = 0.8912
reflections collected	21 792	47 243
independent reflections	4413	9220
reflections obsd	2165 ( <i>I</i> > 3 $\sigma$ )	4428 ( <i>I</i> > $\sigma$ )
refinement on	<i>F</i>	<i>F</i>
<i>R</i>	0.0456	0.0654
<i>R</i> <sub>w</sub>	0.0524	0.0666

parameters for all atoms and anisotropic thermal parameters for non-hydrogen atoms have been deposited at the Cambridge Crystallographic Data Center.

**Theoretical Methods.** The electronic spectra were calculated using the all-valence intermediate neglect of differential overlap (INDO) method,<sup>21</sup> with the open-shell restricted Hartree–Fock (ROHF) formalism. Calculations were performed using the INDO/1 Hamiltonian incorporated in the commercially available MSI software package ZINDO.<sup>22</sup> The monoexcited configuration interaction (MECI) approximation was employed to describe the excited states. The 100 energy transitions between the 10 highest occupied molecular orbitals and the 10 lowest empty ones were chosen to undergo CI mixing. Metrical parameters used for the calculations were taken from the present crystal data. In the case of Cu<sub>2</sub>LO(AcO)·<sup>1</sup>/<sub>2</sub>H<sub>2</sub>O, the calculations reported in the present contribution have been performed on molecule 1 (Cu(101)–Cu(102)). However, we have checked that the calculations qualitatively lead to the same conclusion when performed on molecule 2 (Cu(201)–Cu(202)).

The effect of spin state (*S* = 0 or 1) on the hyperpolarizability was investigated using the Gaussian98 package.<sup>23</sup> The geometry of a model

complex of Cu<sub>2</sub>LO(AcO) (in which the ethyl substituents of the nitrogen atoms have been substituted by hydrogen atoms) has been fully optimized at the B3PW91<sup>24</sup>/6-31G\*/LANL2DZ(Cu) level. The ferromagnetic state (*S* = 1) was calculated at the restricted open spin level whereas the antiferromagnetic complex (*S* = 0) was investigated within Noodleman's broken symmetry (BS) approach.<sup>25</sup> The corresponding static hyperpolarizabilities were calculated at the B3PW91<sup>24</sup>/6-31G\* level using the finite field procedure included in Gaussian98.<sup>26</sup>

**NLO Properties.** The principle of the electric field induced second harmonic (EFISH) technique is reported elsewhere.<sup>27,28</sup> The data were recorded using a picosecond Nd:YAG pulsed (10 Hz) laser operating at  $\lambda$  = 1.064  $\mu$ m. The outcoming Stokes-shifted radiation at 1.907  $\mu$ m generated by Raman effect in a hydrogen cell (1m long, 50 atm.) was used as the fundamental beam for second harmonic generation. The compounds were dissolved in chloroform at various concentrations (0 to 2 × 10<sup>-2</sup> mol L<sup>-1</sup>). The centrosymmetry of the solution was broken by dipolar orientation of the chromophores with a high voltage pulse (around 5 kV) synchronized with the laser pulse. The SHG signal was selected through a suitable interference filter, detected by a photomultiplier, and recorded on an ultrafast Tektronic TDS 620 B oscilloscope. With the NLO response being induced by dipolar orientation of the chromophores, the EFISH signal is therefore proportional to the dipole moment ( $\mu$ ) and to  $\beta_{\text{vec}}$ , the vector component of  $\beta$  along the dipole moment direction. However, due to the symmetry of the present molecules,  $\mu$  and  $\beta_{\text{vec}}$  are parallel and, therefore,  $\beta_{\text{vec}}$  and  $\beta$  are assumed to be equivalent. The dipole moments were measured independently by a classical method based on the Guggenheim theory.<sup>29</sup> Further details of the experimental methodology and data analysis are reported elsewhere.<sup>28</sup>

**Magnetic Measurements.** Magnetic susceptibility data for Cu<sub>2</sub>LO(AcO)·<sup>1</sup>/<sub>2</sub>H<sub>2</sub>O were collected using a SQUID-based magnetometer on a QUANTUM Design Model MPMS instrument. All data were corrected for diamagnetism estimated from Pascal's constants (−322 × 10<sup>-6</sup> cm<sup>3</sup> mol<sup>-1</sup>).<sup>30</sup>

## Results and Discussion

**Synthesis and Characterization.** H<sub>2</sub>LOH is a yellow solid, highly soluble in ethanol, prepared in excellent yield via standard Schiff base condensation. The compound is easily characterized by <sup>1</sup>H NMR. In particular, the appearance of the CH=N signal at 8.03 ppm and the disappearance of the CH=O signal located at 9.47 ppm in the starting diethylaminosalicylaldehyde confirm the completeness of the reaction. Interestingly, the complexation process is driven by the sole stoichiometry and presence of Et<sub>3</sub>N, which leads to very similar thick plates of well-shaped CuLOH·EtOH and Cu<sub>2</sub>LO(AcO)·<sup>1</sup>/<sub>2</sub>H<sub>2</sub>O crystals. The decomposition temperatures of H<sub>2</sub>LOH, CuLOH, and Cu<sub>2</sub>LO(AcO) of 255, 280, and 270 °C, respectively, are satisfactory with respect to the requirement of thermal stability, which has become an important

(20) Watkin, D. J.; Prout, C. K.; Pearce, L. J. *CAMERON*, Chemical Crystallography Laboratory, University of Oxford: Oxford, 1996.

(21) (a) Zerner, M.; Loew, G.; Kirchner, R.; Mueller-Westerhoff, U. *J. Am. Chem. Soc.* **1980**, *102*, 589. (b) Anderson, W. P.; Edwards, D.; Zerner, M. C. *Inorg. Chem.* **1986**, *25*, 2728.

(22) ZINDO, 96.0/4.0.0., Molecular Simulations Inc., 1996.

(23) (a) Frisch, M. J.; Trucks, G. W.; Schlegel, H. B.; Gill, P. M. W.; Johnson, B. G.; M. Robb, M. A.; Cheeseman, J. R.; Keith, T.; Petersson, G. A.; Montgomery, J. A.; Raghavachari, K.; Al-Laham, M. A.; Zakrzewski, V. G.; Ortiz, J. V.; Foresman, J. B.; Cioslowski, J.; Stefanov, B. B.; Nanayakkara, A.; Challacombe, M.; Peng, C. Y.; Ayala, P. Y.; Chen, W.; Wong, M. W.; Andres, J. L.; Replogle, E. S.; Gomperts, R.; Martin, R. L.; Fox, D. J.; Binkley, J. S.; Defrees, D. J.; Baker, J.; Stewart, J. P.; Head-Gordon, M.; Gonzalez, C.; Pople, J. A. *Gaussian 94, Revision E.2*, Gaussian, Inc., Pittsburgh, PA, 1995. (b) Frisch, M. J.; Trucks, G. W.; Schlegel, H. B.; Scuseria, G. E.; Robb, M. A.; Cheeseman, J. R.; Zakrzewski, V. G.; Montgomery, J. A., Jr.; Stratmann, R. E.; Burant, J. C.; Dapprich, S.; Millam, J. M.; Daniels, A. D.; Kudin, K. N.; Strain, M. C.; Farkas, O.; Tomasi, J.; Barone, V.; Cossi, M.; Cammi, R.; Mennucci, B.; Pomelli, C.; Adamo, C.; Clifford, S.; Ochterski, J.; Petersson, G. A.; Ayala, P. Y.; Cui, Q.; Morokuma, K.; Malick, D. K.; Rabuck, A. D.; Raghavachari, K.; Foresman, J. B.; Cioslowski, J.; Ortiz, J. V.; Baboul, A. G.; Stefanov, B. B.; Liu, G.; Liashenko, A.; Piskorz, P.; Komaromi, I.; Gomperts, R.; Martin, R. L.; Fox, D. J.; Keith, T.; Al-Laham, M. A.; Peng, C. Y.; Nanayakkara, A.; Gonzalez, C.; Challacombe, M.; Gill, P. M. W.; Johnson, B.; Chen, W.; Wong, M. W.; Andres, J. L.; Gonzalez, C.; Head-Gordon, M.; Replogle, E. S.; Pople, J. A. *Gaussian 98, Revision A.7*, Gaussian, Inc., Pittsburgh, PA, 1998.

(24) (a) Becke, A. D.; *J. Chem. Phys.* **1993**, *98*, 564. (b) Perdew, J. P.; Wang, Y. *Phys. Rev. B* **1992**, *45*, 13244.

(25) Noodleman, L. *J. Chem. Phys.* **1981**, *74*, 5737.

(26) Rassolov, V.; Pople, J. A.; Ratner, M.; Windus, T. L. *J. Chem. Phys.* **1998**, *109*, 1223. Basis sets were obtained from the Extensible Computational Chemistry Environment Basis Set Database, Version, as developed and distributed by the Molecular Science Computing Facility, Environmental and Molecular Sciences Laboratory which is part of the Pacific Northwest Laboratory, P.O. Box 999, Richland, WA 99352, and funded by the U.S. Department of Energy. The Pacific Northwest Laboratory is a multiprogram laboratory operated by Battelle Memorial Institute for the U.S. Department of Energy under contract DE-AC06-76RLO 1830. Contact David Feller or Karen Schuchardt for further information.

(27) (a) Oudar, J. L. *J. Chem. Phys.* **1977**, *67*, 446. (b) B. F. Levine, C. G. Betha, *J. Chem. Phys.* **1975**, *63*, 2666, and **1976**, *65*, 1989.

(28) Maltey, I.; Delaire, J. A.; Nakatani, K.; Wang, P.; Shi, X.; Wu, S. *Adv. Mater. Opt. Electron.* **1996**, *6*, 233.

(29) Guggenheim, E. A. *Trans. Faraday Soc.* **1949**, *45*, 714.

(30) Earnshaw, A. *Introduction to Magnetochemistry*; Academic Press: London, 1968.

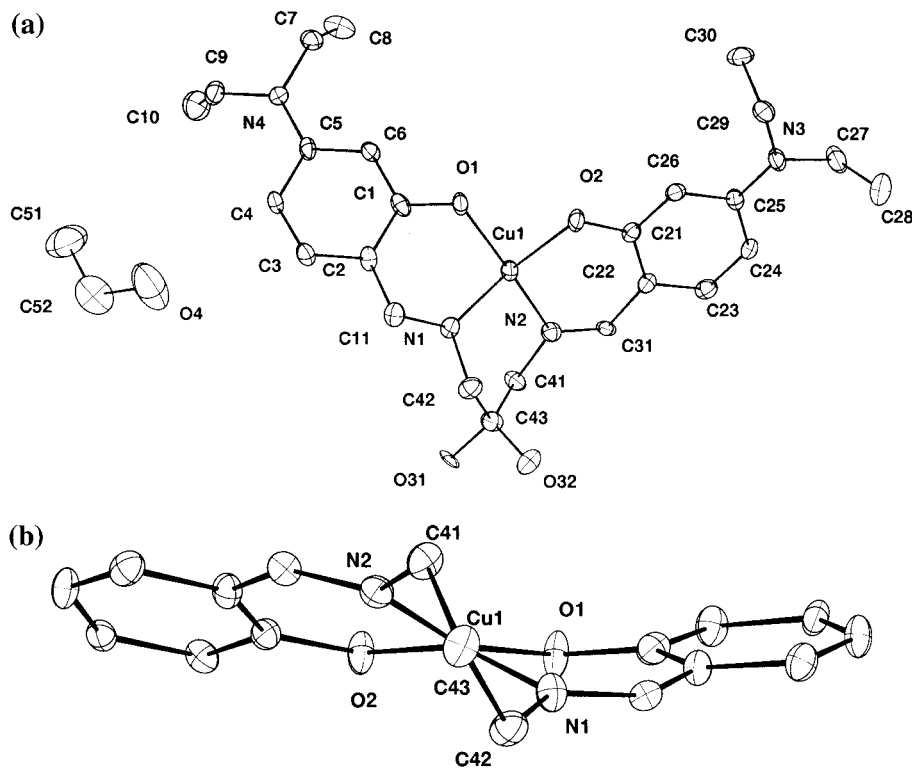


**Figure 1.** (a) Asymmetric unit and atom labeling system for CuLOH·EtOH. H atoms are omitted for clarity. (b) Projection of CuLOH along the C(43)–Cu(1) direction.

**Table 2.** Relevant Metal Ligand Bond Lengths in Å for CuLOH·EtOH and Cu<sub>2</sub>LO(AcO)·½H<sub>2</sub>O

CuLOH·EtOH	Cu <sub>2</sub> LO(AcO)·½H <sub>2</sub> O				
	molecule 1		molecule 2		
Cu(1)–O(1)	1.911(4)	Cu(101)–O(101)	1.878(6)	Cu(201)–O(203)	1.923(6)
Cu(1)–O(2)	1.887(4)	Cu(101)–O(102)	1.921(6)	Cu(201)–O(204)	1.896(6)
Cu(1)–N(1)	1.943(5)	Cu(101)–O(105)	1.908(5)	Cu(201)–O(205)	1.915(6)
Cu(1)–N(2)	1.936(4)	Cu(101)–N(101)	1.917(7)	Cu(201)–N(202)	1.903(7)
		Cu(102)–O(103)	1.943(6)	Cu(202)–O(201)	1.893(6)
		Cu(102)–O(104)	1.892(6)	Cu(202)–O(202)	1.942(6)
		Cu(102)–O(105)	1.914(6)	Cu(202)–O(205)	1.910(6)
		Cu(102)–N(102)	1.913(7)	Cu(202)–N(201)	1.901(7)

prerequisite for NLO chromophores.<sup>31</sup> The role played by the metal center in the alignment of the two donor–acceptor charge-transfer axes of the ligand, and in the enhancement of the thermal stability, has already been pointed out in previous studies.<sup>9,10</sup>

**Structural Studies.** The molecular structure of CuLOH·EtOH is shown in Figure 1a. The asymmetric unit contains one mononuclear complex and a molecule of ethanol. The main metal ligand bond lengths are gathered in Table 2. Contrary to the previously reported structures obtained from the related salen-based ligand,<sup>10d</sup> the metal center is presently located in a rather distorted square planar environment with the angle between the O(1)–Cu(I)–N(1) and O(2)–Cu(1)–N(2) planes equal to 28.38°. Additionally, a view along the Cu(1)–C(43) atoms clearly shows an out-of-plane displacement of the C(41) and C(42) atoms symmetrically from the mean plane defined by the bis(salicylaldehyde)copper(II) skeleton (Figure 1b).

The molecular structure of Cu<sub>2</sub>LO(AcO)·½H<sub>2</sub>O is shown in Figure 2. Two dinuclear species are present in the asymmetric unit, with one molecule of water. The main metal ligand bond lengths are gathered in Table 2 and found to be comparable to those of CuLOH·EtOH with averaged values equal to 1.919(5)

and 1.911(7) Å for the mono- and dimetallic complexes, respectively. Interestingly, Cu<sub>2</sub>LO(AcO)·½H<sub>2</sub>O exhibits more planar geometries than CuLOH·EtOH. For molecule 1, the angles between the O(101)–Cu(101)–N(101) and O(102)–Cu(101)–O(105) planes and between the O(104)–Cu(102)–N(102) and O(103)–Cu(102)–O(105) planes are equal to 11.48° and 6.56°, respectively. For molecule 2, the angles between the O(201)–Cu(201)–N(201) and O(202)–Cu(201)–O(205) planes and between the O(204)–Cu(202)–N(202) and O(203)–Cu(202)–O(205) planes are equal to 2.59° and 8.44°, respectively.

**Spectroscopic Properties.** The optical absorption spectra of CuLOH·EtOH and Cu<sub>2</sub>LO(AcO)·½H<sub>2</sub>O recorded in CH<sub>2</sub>Cl<sub>2</sub> are shown in Figure 3. The spectra exhibit intense bands located in the 300–400 nm domain with absorption maxima ( $\lambda_{\text{max}}$ ) at 353 nm ( $\epsilon = 59\,000\text{ L}^{-1}\text{ mol}^{-1}\text{ cm}^{-1}$ ) and 372 nm ( $\epsilon = 64\,500\text{ L}^{-1}\text{ mol}^{-1}\text{ cm}^{-1}$ ) for CuLOH·EtOH and Cu<sub>2</sub>LO(AcO)·½H<sub>2</sub>O, respectively. Additional transitions can be evidenced as shoulders in the figure. For comparison, the spectrum of H<sub>2</sub>LOH is also provided ( $\lambda_{\text{max}} = 343\text{ nm}$ ,  $\epsilon = 62\,800\text{ L}^{-1}\text{ mol}^{-1}\text{ cm}^{-1}$ ). The spectra clearly reveal a red shift upon metal complexation, which seems to be a trend in donor–acceptor salen complexes.<sup>9,10</sup> This effect is more pronounced for the dinuclear compound. Interestingly, both complexes exhibit a slightly

(31) Dagani, R. *Chem. Eng. News* **1996**, March 4, 22.

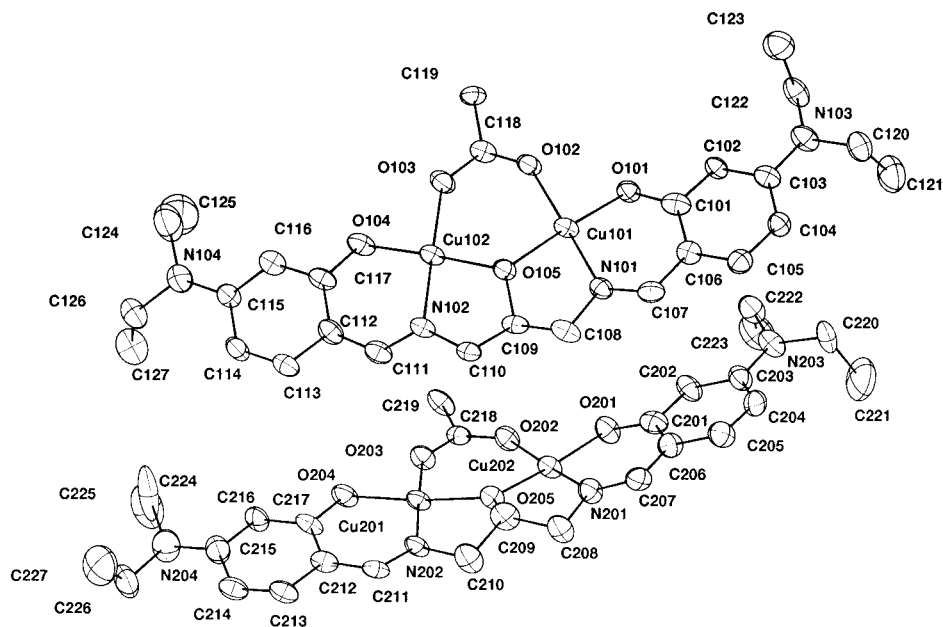


Figure 2. Atom labeling for molecules 1 (top) and 2 (bottom) in the asymmetric unit of  $\text{Cu}_2\text{LO}(\text{AcO}) \cdot \frac{1}{2}\text{H}_2\text{O}$ .

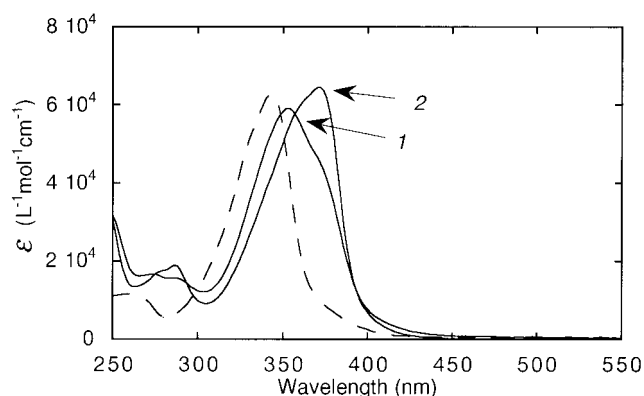


Figure 3. Optical spectra for  $\text{CuLOH}$  (1) and  $\text{Cu}_2\text{LO}(\text{AcO})$  (2) in  $\text{CH}_2\text{-Cl}_2$  vs that of the  $\text{H}_2\text{LOH}$  ligand (dotted line).

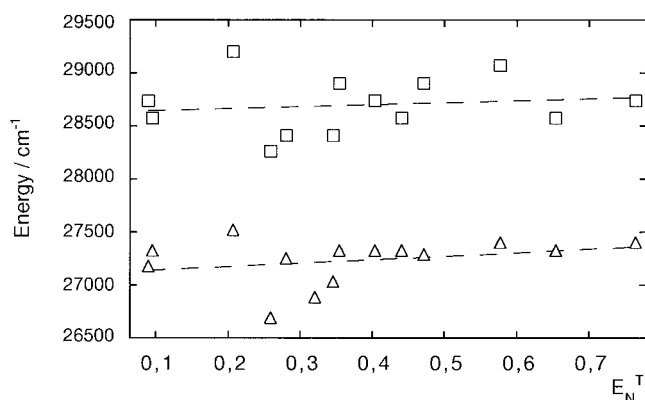


Figure 4. Solvatochromism (energy in  $\text{cm}^{-1}$ ) for  $\text{Cu}_2\text{LO}(\text{AcO})$  (triangles) and  $\text{CuLOH}$  (squares) plotted vs the Reichardt empirical parameter ( $E_T^N$ ).

negative solvatochromism (red shift as the solvent polarity decreases). These behaviors are compared in Figure 4 where the absorption maxima (in  $\text{cm}^{-1}$ ) are drawn vs the Reichardt solvent parameter  $E_T^N$ .<sup>32</sup> Solvatochromism is usually indicative of changes occurring in dipole moments between the ground and excited states upon excitation ( $\Delta\mu < 0$  in the case of

Table 3. Experimental and ZINDO-Computed Data for the High Intensity Optical Transitions of  $\text{CuLOH}$  and  $\text{Cu}_2\text{LO}(\text{AcO})$

	$\lambda$ in nm		intensity	
	calcd (transition no.)	exp	calcd (f)	exp ( $\epsilon$ ) in $\text{L}^{-1} \text{mol}^{-1} \text{cm}^{-1}$
$\text{CuLOH}$	312 (1 → 15)	353	0.69	59 000
	341 (1 → 9)	370–380	0.45	sh
$\text{Cu}_2\text{L}(\text{AcO})$	349 (1 → 12)	372	0.87	64 450
	396 (1 → 9)	355–365	0.30	sh
	404 (1 → 8)		0.29	

negative solvatochromism), and therefore potential NLO capabilities (vide infra). The slopes in Figure 4 are equal to 180 and 320, for the mono- and the dinuclear species, respectively. Therefore, the present data suggest that the solvatochromic shift is more pronounced for  $\text{Cu}_2\text{LO}(\text{AcO}) \cdot \frac{1}{2}\text{H}_2\text{O}$  than for  $\text{CuLOH} \cdot \text{EtOH}$ , which might provide experimental evidences for larger  $\Delta\mu$  in the dinuclear species. However, it is difficult to conclude nonambiguously, taking into account the important discrepancy observed in the data gathered in Figure 4. Furthermore, it has also been mentioned here that experimental estimation of  $\Delta\mu$  by means of solvatochromic shifts may not be fully reliable in some cases.<sup>33</sup>

The ZINDO spectra have been calculated for  $\text{CuLOH}$  and  $\text{Cu}_2\text{LO}(\text{AcO})$ . In both cases, the spectra are dominated by an intense transition ( $\lambda_{\text{max}}$ ), namely, 1 → 15 and 1 → 12 for  $\text{CuLOH}$  and  $\text{Cu}_2\text{LO}(\text{AcO})$ , respectively. Additional, but less intense, transitions are present at lower energies. The calculated data are compared to the experimental values in Table 3. The agreement appears satisfactory, with an experimental spectrum slightly red shifted (30–40 nm) in the case of  $\text{CuLOH}$ . On passing from the mono- to the dinuclear species, a tendency for higher absorption maximum ( $\lambda_{\text{max}}$ ) and higher oscillator strength is evidenced in full agreement with the experiment. By contrast, the energy of the shoulder disagrees with that found

(33) See, for example: (a) Alain, V.; Rédoglia, S.; Blanchard-Desce, M.; Lebus, S.; Lukaszuk, K.; Wortmann, R.; Gubler, U.; Bosshard, C.; Günter, P. *Chem. Phys.* **1999**, *245*, 51. (b) Blanchard-Desce, M.; Alain, V.; Midrier, L.; Wortmann, R.; Lebus, S.; Glania, C.; Kramer, P.; Fort, A.; Müller, J.; Barzoukas, M. *J. Photochem. Photobiol. A* **1997**, *195*, 115. (c) Lacroix, P. G.; Malfant, I.; Iftime, G.; Razus, A. C.; Nakatani, K.; Delaire, J. A. *Chem. Eur. J.* **2000**, *6*, 2599.

(32) Reichardt, C.; Harbush-Görmet, E. *Liebigs Ann. Chem.* **1983**, *5*, 721.

**Table 4.** EFISH Data ( $\mu \times \beta$  in D cm<sup>5</sup> esu<sup>-1</sup>), Dipole Moments ( $\mu$  in D), and Hyperpolarizabilities ( $\beta$  in cm<sup>5</sup> esu<sup>-1</sup>) for CuLOH·EtOH and Cu<sub>2</sub>LO(AcO)<sup>1/2</sup>H<sub>2</sub>O at 1.907  $\mu$ m

	$\mu \times \beta$	$\mu$	$\beta$
CuLOH·EtOH	$-9.5 \times 10^{-30}$	1.6	$-5.9 \times 10^{-30}$
Cu <sub>2</sub> LO(AcO) <sup>1/2</sup> H <sub>2</sub> O	$-51 \times 10^{-30}$	4.7	$-10.9 \times 10^{-30}$

by experiment for Cu<sub>2</sub>LO(AcO). However, the transitions associated with these shoulders will be found to contribute very little to the NLO response for both copper complexes (vide infra). Therefore, this discrepancy should have a limited effect on the estimation of the hyperpolarizabilities.

**NLO Properties of Cu<sub>2</sub>LO(AcO) vs CuLOH.** CuLOH and Cu<sub>2</sub>LO(AcO) belong to a class of thermally stable Schiff base complexes which have previously been identified as potential NLO candidates in relation to their ability to be incorporated into a pooled polymer matrix.<sup>9,10</sup> In this approach, which has become the most popular strategy toward efficient NLO materials, the parameter of merit is the  $\mu \times \beta$  product, measured by the EFISH technique. The EFISH data are summarized in Table 4.

Interestingly, the formal addition of one Cu<sup>II</sup>-AcO<sup>-</sup> unit results in a 5 $\times$  enhancement of the NLO response on passing from CuLOH to Cu<sub>2</sub>LO(AcO), although both molecules possess the same  $\pi$ -electronic core. The table reveals that a larger dipole moment in the dinuclear species probably accounts for most of this effect. However, the hyperpolarizability still undergoes a sizable experimental enhancement (83%), which can tentatively be related to the electronic transitions of the molecules.

Within the framework of the sum over state (SOS) perturbation theory,  $\beta$  can be related to all excited states of a molecule.<sup>34</sup> In the case of bis(salicylaldiminato) Schiff bases complexes, various previous reports<sup>9,10</sup> have pointed out that the nonlinearity is dominated by a contribution so-called "two-level term" according to the following relation:<sup>27a</sup>

$$\beta_{xxx} = \sum_i \frac{3e^2 \hbar f \Delta\mu}{2m(\Delta E)^3} \times \frac{(\Delta E)^4}{((\Delta E)^2 - (2\hbar\omega)^2)((\Delta E)^2 - (\hbar\omega)^2)} \quad (1)$$

in which  $\hbar\omega$  is the energy of the incident laser beam and  $\beta_{xxx}$  the principal tensor component along the dipolar axis. Equation 1 indicates that any transition ( $i$ ) of high intensity (oscillator strength  $f$ ), large dipole moment change ( $\Delta\mu$ ), and low energy ( $\Delta E$ ) will significantly contribute to  $\beta$ . Unfortunately, the calculation cannot be carried out for open-shell chromophores using the present ZINDO release; therefore  $\beta$  cannot be fully evaluated using this formalism. Nevertheless, a qualitative description of the origin of the NLO response can tentatively be conducted on the basis of a simplified two-level model, when the summation in eq 1 can be reduced to a single component, exhibiting large  $f$  and  $\Delta\mu$  values and low energy ( $\Delta E$ ).

The eigenvalues and population analysis of the relevant ZINDO calculated MOs are compiled in Table 5. The 92 MO represents the unpaired electron and is strongly localized in the copper(II) atom for CuLOH, while 108 and 109 MOs are the corresponding semioccupied MOs for Cu<sub>2</sub>LO(AcO). Note that these partially filled orbitals do not represent the HOMO but are more stable than several double occupied ligand orbitals. This aspect has been addressed theoretically<sup>35</sup> and is a common feature of SCF calculations of many transition metal complexes

**Table 5.** Energies (eV) and Population Analysis (%) of the Relevant MOs for CuLOH and Cu<sub>2</sub>LO(AcO)

MO	energy	population					character
		Cu	phenyl	O <sub>phenol</sub>	NET <sub>2</sub>	C=N	
CuLOH							
94	-0.160	1	38	3	3	55	$\pi^*$
93	-0.169	0	41	2	3	53	$\pi^*$
92	-8.803	66	2	17	0	14	d
91	-7.181	1	54	4	25	14	$\pi$
90	-7.266	1	53	1	32	12	$\pi$
89	-7.720	2	65	22	10	0	$\pi$
88	-7.834	2	69	22	7	1	$\pi$
Cu <sub>2</sub> LO(AcO)							
111	-1.017	0	38	2	2	55	$\pi^*$
110	-1.047	1	38	2	2	55	$\pi^*$
109	-9.029	64	1	10	0	10	d
108	-9.589	68	1	10	0	8	d
107	-7.641	1	55	4	22	16	$\pi$
106	-7.687	2	57	5	19	16	$\pi$
105	-7.924	1	71	14	14	0	$\pi$
104	-7.962	1	69	13	16	0	$\pi$

with partially filled metal-d orbitals.<sup>36</sup> After CI mixing, the features of the main resulting transitions for CuLOH and Cu<sub>2</sub>LO(AcO) are gathered in Table 6. In the case of CuLOH, the 1  $\rightarrow$  15 transition has an  $f \times \Delta\mu/(\Delta E)^3$  factor 2.2 times that of 1  $\rightarrow$  9. This ratio reaches 3.7 (3.8) between 1  $\rightarrow$  12 and 1  $\rightarrow$  8 (1  $\rightarrow$  9) for Cu<sub>2</sub>LO(AcO). Therefore, and with respect to eq 1, the high-intensity transitions are the dominant electronic features accounting for most of the NLO response for both complexes. Following the earlier ZINDO analysis of the NLO response of organotransition metal complexes by Marks and Ratner,<sup>37</sup> we make here the assumption that understanding the changes occurring for these transitions on passing from the mono- to the dinuclear species can provide a qualitative understanding of the origin of the experimental  $\beta$  enhancement evidenced in the dinuclear system.

For the sake of simplification, a molecular 2-fold axis will be assumed in the following section to describe the charge transfer in CuLOH and Cu<sub>2</sub>LO(AcO). In the case of CuLOH, the composition of the 1  $\rightarrow$  15 transition involves two main components ( $\chi_{88 \rightarrow 93}$  and  $\chi_{89 \rightarrow 94}$ ) related by symmetry, each of them involving one side of the ligand. The differences in electronic populations associated with these transitions are shown in Figure 5, with the resulting charge transfers (arrows in figure). It appears that most of the behavior is dominated by the ligand. Projection along the symmetry (OX) axis yields the resulting dipole moment change  $\Delta\mu = \Delta\mu_x = -9.2$  D for the 1  $\rightarrow$  15 transition.

It is interesting to note that the charge transfer observed in CuLOH seems to have its counterpart in Cu<sub>2</sub>LO(AcO). In particular, the main components of the dominant 1  $\rightarrow$  12 transition are associated with intraligand charge transfers. It can be observed that changing the nature of the inorganic core may have the potential of modulating the magnitude and direction of the charge transfer, and hence the value of  $\Delta\mu$  (Figure 5). Nevertheless, the modulation in magnitude and direction tend to compensate each other in the present case, and the resulting  $\Delta\mu$  value of  $-9.3$  D is only slightly enhanced in Cu<sub>2</sub>LO(AcO).

(36) See, for example: (a) Di Bella, S.; Lanza, G.; Gulioni, A.; Fragalà, I. *Inorg. Chem.* **1996**, *35*, 5, 3885. (b) Di Bella, S.; Lanza, G.; Fragalà, I.; Marks, T. J. *Organometallics* **1996**, *15*, 5, 205. (c) Di Bella, S.; Gulino, A.; Lanza, G.; Fragalà, I.; Marks, T. J. *J. Phys. Chem.* **1993**, *97*, 11673.

(37) See for example: (a) Kanis, D. R.; Ratner, M. A.; Marks, T. J. *J. Am. Chem. Soc.* **1992**, *114*, 10338. (b) Kanis, D. R.; Lacroix, P. G.; Ratner, M. A.; Marks, T. J. *J. Am. Chem. Soc.* **1994**, *116*, 10089.

(34) Ward, J. F. *Rev. Mod. Phys.* **1965**, *37*, 1.

(35) For an accurate analysis of this phenomena, see: Ferreira, R. *Struct. Bonding (Berlin)* **1976**, *31*, 1.

**Table 6.** Energies ( $\lambda_{\text{Max}}$  in nm), Oscillator Strengths ( $f$ ), Dipole Moments Changes ( $\Delta\mu$  in D),  $f \times \Delta\mu/(\Delta E)^3$  Factor (Arbitrary Unit), and Composition of the Excited States for the High-Intensity Electronic Transitions of CuLOH and Cu<sub>2</sub>LO(AcO)

compound	transition	$\lambda_{\text{max}}$	$f$	$\Delta\mu^a$	$(f \times \Delta\mu)/(\Delta E)^3$	composition of CI expansion <sup>b</sup>
CuLOH	1 → 9	341	0.45	-5.0	0.26	$0.46\chi_{91-93} - 0.36\chi_{90-94}$
	1 → 15	312	0.69	-9.2	0.56	$0.50\chi_{88-93} + 0.46\chi_{89-94}$
Cu <sub>2</sub> LO(AcO)	1 → 8	404	0.29	-4.9	0.27	$-0.48\chi_{106-110} + 0.44\chi_{107-111}$
	1 → 9	396	0.30	-4.9	0.26	$0.52\chi_{106-110} + 0.51\chi_{107-111}$
	1 → 12	349	0.87	-9.3	1.00	$0.56\chi_{105-111} + 0.44\chi_{104-110}$

<sup>a</sup> Calculated using the two dominant transitions of the CI compositions, in each case. The dipole moments are oriented along the pseudo-2-fold axis of the molecules (Figure 5). <sup>b</sup> Orbital 92 is the SOMO and orbital 93 the LUMO for CuLOH. Orbitals 108 and 109 are the SOMO and orbital 110 the LUMO for Cu<sub>2</sub>LO(AcO).

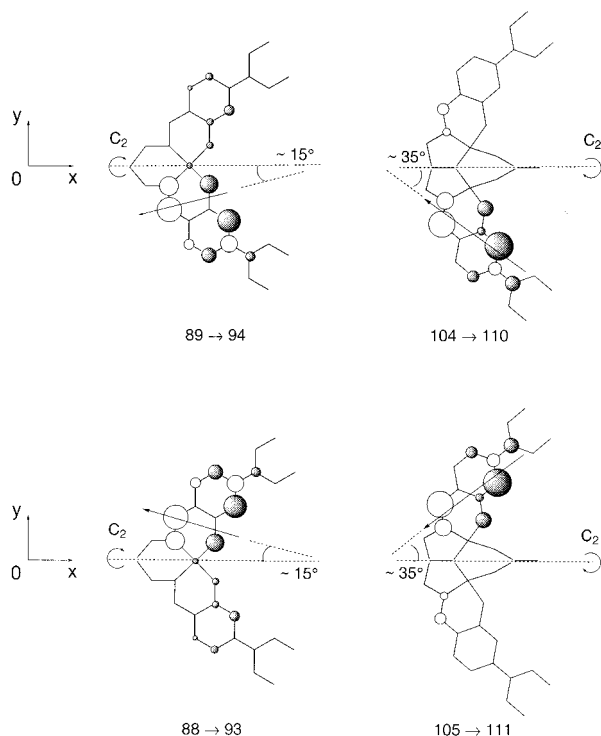


**Figure 5.** Difference in electronic populations between ground and excited states for the main transitions (1 → 15 and 1 → 12) involved in the NLO response of CuLOH (left) and Cu<sub>2</sub>LO(AcO) (right), respectively. The white (black) contribution is indicative of an increase (decrease) of electron density in the charge-transfer process. The arrows indicate the direction of the charge transfer associated with the transitions, and the dotted lines indicate the pseudo-2-fold axis of the molecules.

This  $\Delta\mu$  enhancement is qualitatively consistent with the experimental solvatochromic behavior observed in both complexes (Figure 4). A more important effect appears to be associated with the slight red shift and enlarged oscillator strength. Within the framework of the two-level description of  $\beta$  (eq 1), the combination of the changes occurring on  $\Delta\mu$ ,  $f$ , and  $\Delta E$  (Table 6) lead to an 85% enhancement of the hyperpolarizability on passing from the mono- to the dinuclear species, which must be compared to the experimental 83% enhancement of  $\beta$ . The agreement between experiment and calculation is excellent. However, it must be pointed out that, owing to the crude approximations imposed by the two-level analysis, such a perfect agreement is probably somewhat fortuitous.

**Cu<sub>2</sub>LO(AcO)·1/2H<sub>2</sub>O: A Multifunctional Material?** Magnetic susceptibility data for a solid powdered sample of Cu<sub>2</sub>LO(AcO)·1/2H<sub>2</sub>O are displayed in Figure 6 as a plot of  $\chi \times T$  vs  $T$ , with  $\chi$  being the molar magnetic susceptibility and  $T$  the temperature. At room temperature, the  $\chi \times T$  product is equal to 0.55 cm<sup>3</sup> K mol<sup>-1</sup>, as expected for two weakly interacting

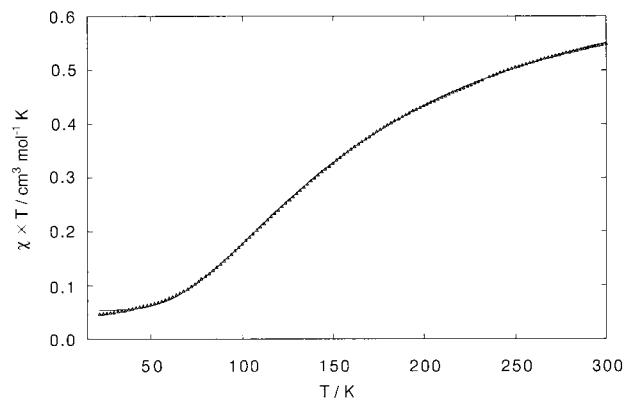


**Figure 6.** Experimental (triangles) and calculated (straight line) temperature dependence of the  $\chi \times T$  product for Cu<sub>2</sub>LO(AcO)·1/2H<sub>2</sub>O.

magnetic centers with  $S = 1/2$ .  $\chi$  reaches a maximum at 170 K and then decreases as the temperature is lowered, a behavior indicative of an intramolecular antiferromagnetic coupling between the copper(II) centers. The magnetic properties can readily be ascribed to an antiferromagnetic coupling between  $S = 1/2$  metal centers, according to the following expression:<sup>38</sup>

$$\chi = (1 - \rho) \left( \frac{2N\mu_B^2 g^2}{kT} \times \frac{1}{3 + \exp\left(\frac{-J}{kT}\right)} \right) + \rho \left( \frac{N\mu_B^2 g^2}{2kT} \right) \quad (2)$$

where  $N$  is Avogadro's number,  $g$  is the Zeeman splitting parameter,  $\mu_B$  is the Bohr magneton,  $k$  is the Boltzmann constant, and  $J$  is the singlet-triplet energy gap ( $E_{S=0} - E_{S=1}$ ).  $\rho$  is the proportion of noncoupled impurity, the susceptibility of which is assumed to follow the Curie law ( $\chi = C/T$ ). The least-squares best fit is found for  $J = -207.7$  cm<sup>-1</sup>,  $g = 2.018$ , and  $\rho = 0.071$ . The discrepancy factor defined as  $R(\chi) = \sum(\chi_{\text{obs}} - \chi_{\text{calc}})^2 / \sum(\chi_{\text{obs}})^2$  is equal to  $3.7 \times 10^{-6}$ . The slight discrepancy observed at low temperature between experimental and theoretical data (Figure 6) might tentatively be related to the presence of additional intermolecular magnetic interaction. Several dinuclear copper(II) metal complexes have been reported in the literature, with one bridge an alkoxo and the other one an exogenous acetate.<sup>39,40</sup> Contrary to symmetric alkoxo-bridged dimers, which usually lead to very high coupling constant values (e.g.,  $-J > 500$  cm<sup>-1</sup> in phenolato-bridges systems),<sup>41</sup> the situation in which one bridge is an alkoxo and the other one a carboxylato leads to reduced coupling constants. In this respect, the present  $J =$

(38) Bleaney, B.; Bowers, K. D. *Proc. R. Soc. (London)* **1952**, A214, 451.

(39) Nishita, Y.; Kida, S. *J. Chem. Soc., Dalton Trans.* **1986**, 2633.

(40) Mazurek, W.; Kennedy, B. J.; Murray, K. S.; O'Connor, M. J.; Rodgers, J. R.; Snow, M. R.; Wedd, A. G.; Zwack, P. R. *Inorg. Chem.* **1985**, 24, 3258.

(41) Mandal, S. K.; Thompson, L. K.; Newlands, M. J.; Gabe, E. J.; Nag, K. *Inorg. Chem.* **1990**, 29, 1324 and references herein.

$-207.7 \text{ cm}^{-1}$  value is consistent with the values previously reported.<sup>39,40</sup>

The presence of a dinuclear complex, which exhibits both magnetic and NLO behaviors, raises the question of a possible interaction between the properties at the molecular level. Multiproperty molecular materials are of growing interest, in relation to the emerging concept of molecular switches.<sup>42</sup> At the synthetic level, it is interesting to note that the presence of amine leads to the transformation of the mono- to the dinuclear species and to a  $5\times$  enhancement of the  $\mu \times \beta$  product. This might be seen as a potential NLO switch, although the reversibility and practical use of this effect would be questionable. At a more theoretical level, the possibility of NLO modulation occurring upon spin transition has recently been pointed out in mononuclear species.<sup>16,43</sup> Along this line, one may wonder if the hyperpolarizability of magnetically coupled NLO chromophores could exhibit a spin dependence in some cases. To test this possibility, a calculation has been conducted within the framework of the DFT theory, which can provide a value of the hyperpolarizability using the finite field (FF) procedure. In this approach,  $\beta$  is obtained as the numerical partial derivative of the energy ( $W$ ) with respect to the electric field ( $E$ ), evaluated at zero field according to the following equation:

$$\beta_{ijk} = -\left(\frac{\partial^3 W}{\partial E_i \partial E_j \partial E_k}\right)_{E=0} \quad (3)$$

an expression which is only valid for the static field limit.<sup>44</sup> Following this approach,  $\beta$  is the magnitude of the vectorial hyperpolarizability ( $\beta = \sqrt{(\beta_x)^2 + (\beta_y)^2 + (\beta_z)^2}$ ) with  $\beta_i = \beta_{ixx} + \beta_{iyy} + \beta_{izz}$  after assumption of the Kleinman symmetry conditions.<sup>45</sup> The energy gap between the triplet state and the BS state of the model complex is equal to  $431 \text{ cm}^{-1}$  and must be compared to the experimental  $J/2$  value<sup>46</sup> of  $104 \text{ cm}^{-1}$ . The relative order of both spin states is satisfactory. However, the energy gap is overestimated as compared to the experimentally measured one. This tendency of DFT has already been pointed out by Illas et al.<sup>47</sup> This discrepancy may also be related to the use of a model instead of the real copper complex. The hyperpolarizabilities have been calculated for both spin states. The  $\beta$  values have been found equal to  $-22.15$  and  $-22.20 \times 10^{-30} \text{ cm}^5 \text{ esu}^{-1}$  for the singlet and triplet states, respectively. At first, the comparison between the DFT-calculated  $\beta$  and the

experimental  $-10.6 \times 10^{-30} \text{ cm}^5 \text{ esu}^{-1}$  value reveals an important discrepancy. However, it is noteworthy that significant differences in the magnitude of the experimental and calculated hyperpolarizabilities may be observed in some cases. In particular, we have previously observed a tendency for overestimating  $\beta$  within the framework of the DFT theory.<sup>15,16</sup> Moreover, the 6-31G\* basis set used here for hyperpolarizability calculations does not include diffuse functions, as usually required to obtain  $\beta$  values of meaningful quality.<sup>44</sup> Due to the size of the molecule, using the 6-31+G\* basis set results in a computational cost that is too high. Nevertheless, it may be expected that in our calculation conditions a comparison of the relative  $\beta$  values of the singlet and triplet states is meaningful. Therefore, the data reveals that the hyperpolarizability is not significantly affected by the spin state in the present case. The fact that the d orbital core is weakly involved in the charge-transfer process in  $\text{Cu}_2\text{LO}(\text{AcO})$ , as anticipated from the examination of Figure 5, probably accounts for this result. One might suppose that a convincing spin dependence of  $\beta$  would rather require metal complexes with more efficient metal–ligand charge-transfer capabilities.

### Conclusion

$\text{CuLOH}$  and  $\text{Cu}_2\text{LO}(\text{AcO})$  are two thermally stable NLO chromophores. The presence of amine leads to the transformation of the mono- to the dinuclear species, with the observation of a NLO switch having a  $\mu \times \beta$  value  $5\times$  larger in  $\text{Cu}_2\text{LO}(\text{AcO})$  than in  $\text{CuLOH}$ . Besides an increased dipole moment, the  $\beta$  enhancement observed on passing from the mono- to the dinuclear species is rationalized by a ZINDO analysis, in terms of red shift and increased oscillator strength. Up to now, the design of polynuclear species with NLO capabilities has received little attention and has focused on diamagnetic systems.<sup>48,49</sup> The present report suggests that magnetically coupled polynuclear chromophores could be envisioned as well to provide NLO chromophores with extended electronic properties. However, the d orbital core of the metal centers is weakly involved in the charge-transfer process for the present copper(II) complexes, and the magnetic coupling leads to no appreciable change in the magnitude of the hyperpolarizability.

**Acknowledgment.** The authors thank CALMIP (CALcul en MIdi Pyrénées–Toulouse, France) for parallel computing facilities, the Groupement de Recherche CNRS Matériaux et Fonction de l'Optique non lineaire for a financial support, Professor H. Chermette and Professor S. Di Bella for fruitful discussions, and Dr. A. Mari for his aid with the magnetic measurements.

**Supporting Information Available:** X-ray materials (atomic coordinates, full interatomic distances and bond angles) and 15 molecular orbitals. This material is available free of charge via Internet at <http://pubs.acs.org>.

IC0013429

- (42) (a) Lehn, J.-M. *Supramolecular Chemistry – Concepts and Perspectives*; VHC: Weinheim, 1995. (b) Warfd, M. D. *Chem. Soc. Rev.* **1995**, 24, 121.
- (43) (a) Létard, J.-F.; Montant, S.; Guionneau, P.; Martin, P.; Le Calvez, P.; Le Calvez, A.; Freysz, E.; Chasseau, D.; Lapouyade, R.; Kahn, O. *Chem. Commun.* **1997**, 745. (b) Gaudry, J. B.; Capes, L.; Langot, P.; Marcén, S.; Kollmannsberger, M.; Lavastre, O.; Freysz, E.; Létard, J.-F.; Kahn, O. *Chem. Phys. Lett.* **2000**, 324, 321.
- (44) Kanis, D. R.; Ratner, M. A.; Marks, T. J., in ref 2c, p 195.
- (45) Kleinman, D. A. *Phys. Rev.* **1962**, 126, 1977.
- (46) Noodleman, L.; Peng, C. Y.; Case, D. A.; Mousesca, J.-M. *Coord. Chem. Rev.* **1995**, 144, 199.
- (47) (a) Caballol, R.; Castell, O.; Illas, F.; Moreira, I. de P. R.; Malrieu, J. P. *J. Phys. Chem. A* **1997**, 101, 7860. (b) Cabrero, J.; Ben Amor, N.; de Graaf, C.; Illas, F.; Caballol, R. *J. Phys. Chem. A* **2000**, 9983.

- (48) Buey, J.; Coco, S.; Díez, L.; Espinet, P.; Martín-Alvarez, J. M.; Miguel, J. A.; García-Granda, S.; Tesouro, A.; Ledoux, I.; Zyss, J. *Organometallics* **1998**, 17, 1750.
- (49) For a recent review of mono and bimetallic NLO species, see: Whittall, I. R.; McDonagh, A. M.; Humphrey, M. G.; Samoc, M. *Adv. Organomet. Chem.* **1998**, 42, 291.